Available online at www.sciencedirect.com

ScienceDirect

Biochimica et Biophysica Acta 1783 (2008) 312–322

Biochimica et Biophysica Acta BBA

www.elsevier.com/locate/bbamcr

Cystatin B and its EPM1 mutants are polymeric and aggregate prone *in vivo*

Elena Cipollini [a], Massimo Riccio [b], Rossella Di Giaimo [c], Fabrizio Dal Piaz [d], Giuseppe Pulice [a], Sandra Catania [a], Ilaria Caldarelli [c], Maja Dembic [e], Spartaco Santi [e], Marialuisa Melli [a,*]

[a] *Department of Biology, University of Bologna, Via Selmi 3, 40126 Bologna, Italy*
[b] *Department of Anatomy and Histology, University of Modena and Reggio Emilia, Largo Del Pozzo 71, 41100 Modena, Italy*
[c] *Department of Biological Sciences, Federico II University, Via Mezzocannone 8, 80134, Naples, Italy*
[d] *Department of Farmaceutical Sciences, University of Salerno, Via Ponte Don Melillo, 84084 Fisciano (SA), Italy*
[e] *Institute of Organ Transplantation and Immunocitology-ITOI, C.N.R c/o I.O.R., 40136 Bologna, Italy*

Received 6 July 2007; received in revised form 13 August 2007; accepted 15 August 2007
Available online 4 September 2007

Abstract

Progressive myoclonus epilepsy type 1 (EPM1) is a neurodegenerative disease correlating with mutations of the cystatin B gene. Cystatin B is described as a monomeric protein with antiprotease function. This work shows that, *in vivo*, cystatin B has a polymeric structure, highly resistant to SDS, urea, boiling and sensitive to reducing agents and alkaline pH. Hydrogen peroxide increases the polymeric structure of the protein. Mass spectrometry analysis shows that the only component of the polymers is cystatin B. EPM1 mutants of cystatin B transfected in cultured cells are also polymeric. The banding pattern generated by a cysteine-minus mutant is different from that of the wild-type protein as it contains only monomers, dimers and some very high MW bands while misses components of MW intermediate between 25 and 250 kDa. Overexpression of wild-type or EPM1 mutants of cystatin B in neuroblastoma cells generates cytoplasmic aggregates. The cysteine-minus mutant is less prone to the formation of inclusion bodies. We conclude that cystatin B *in vivo* has a polymeric structure sensitive to the redox environment and that overexpression of the protein generates aggregates. This work describes a protein with a physiological role characterized by highly stable polymers prone to aggregate formation *in vivo*.

Keywords: Polymers; Cystatin B; Cellular aggregates; EPM1; Neurodegeneration; Cytoskeleton

Cystatin B (CSTB) was first described as an inhibitor of the cysteine family of proteases [1–3]. Its biochemical properties have been studied in depth and its activity characterized [4–6]. The crystal structure of the protein in complex with papain [7], its domain-swapped dimeric [8] and tetrameric forms [9] have been determined. Although the antiprotease activity of CSTB has been demonstrated, there is evidence implying that this may not be the only function. Di Giaimo et al. [10], in rat, have isolated a number of proteins interacting specifically with CSTB, none of which is a protease. The interactors are cytoplasmic proteins involved in cytoskeletal function. Some of them are expressed exclusively in neurons. A specific function of CSTB in the central nervous system may correlate with a recent observation by Riccio et al. [11] showing cell-specific expression of CSTB in the cerebellum, restricted to Purkinje cells and Bergmann glial fibers.

Additional evidence on multiple functions of CSTB comes from the involvement of cystatins in cancer [12], inflammation [13], native immunity [14] and from their presence in the amyloid plaques of Alzheimer's, Parkinson's diseases and spongiform encephalopathies [15]. Increased cystatins A and B in the plaques of Alzheimer's and Parkinson's diseases, and of patients suffering from senile dementia is a common finding and

Abbreviations: aa, amino acid; abs, antibodies; CSTB, cystatin B; cstb, cystatin B gene; EPM1, progressive myoclonus epilepsy type 1; ip, immunoprecipitate; MW, molecular weight; wt, wild type; IPTG, isopropyl-beta-D-thiogalactopyranoside; HA, hemagglutinin; SDS-PAGE, sodium duodecylsulphate-polyacrylamide gel electrophoresis; DTT, dithiothreitol; PBS, phosphate-buffered saline; EDTA, ethylenediamine-tetraacetic acid; NP40, Nonidet P-40; GSH, reduced glutathione; β-METOH, mercaptoethanol; GAPDH, glyceraldehyde-3-phosphate dehydrogenase; EGFP, enhanced green fluorescent protein

* Corresponding author. Tel.: +39 051 2094146; fax: +39 051 2094286.
E-mail address: marialuisa.melli@unibo.it (M. Melli).

0167-4889/$ - see front matter © 2007 Elsevier B.V. All rights reserved.
doi:10.1016/j.bbamcr.2007.08.007

suggests that they are amyloid constituents [15,16]. Interestingly, proteins of the cystatin family are used as models for *in vitro* studies of amyloid fiber structure [17–19] and Staniforth et al. [20], Janowski et al. [8] and Sanders et al. [21] have determined the 3D structure of highly stable domain-swapped dimers *in vitro*. If polymerization of cystatins exists *in vivo*, it may be important for function(s) other than the inhibition of proteinases.

The most studied pathology characterized by mutations of the *cstb* gene is progressive myoclonus epilepsy of the Unverricht–Lundborg type (EPM1) [22]. EPM1 is an autosomal recessive disorder in which patients suffer from myoclonic jerks, frequent tonic–clonic seizures, and progressive decline in cognition [6]. The autoptic results of pathologists on the brain of the deceased patients show neural degeneration in several areas of the central nervous system with cerebellar damage and serious alterations of the Purkinje cells [23]. Although the *cstb* gene is responsible for the disease, recently, cases have been described that carry mutations associated with genes located on different chromosomes [6,24,25].

The most common mutation described in EPM1 patients is the expansion of an unstable dodecamer in the *cstb* promoter [26,27]. This sequence, repeated up to 75 times, is found in homozygosis or in heterozygosis together with an allele carrying one of the following point mutations. A G4R or Q71P substitution, three splice site mutations altering the intron–exon junctions of the gene, a translational stop codon at amino acid position 68 (Δ68), and a frameshift at position 72, followed by a termination codon at position 75 (Δtc) [6,28].

This work shows that CSTB has a polymeric structure *in vivo* in human and rat cells and, when overexpressed, generates cellular aggregates. We propose that the regulation of both expression and polymerization of CSTB is very critical for the cell and that a deregulation event may induce neural degeneration.

1. Material and methods

1.1. Antibodies (abs)

Rabbit anti-CSTB polyclonal abs, Biogenesis; mouse anti-GAPDH monoclonal abs (MAB374), Chemicon; mouse anti-HA (F-7) monoclonal abs and rabbit anti-HA (Y11) polyclonal abs, Santa Cruz Biotechnology, HRP-conjugated goat anti-mouse IgG and goat anti-rabbit IgG, Santa Cruz Biotechnology; FITC-conjugated sheep anti-mouse abs F(ab′)2 fragment, Sigma; CyTM5-conjugated donkey anti-rabbit abs F(ab′)2 fragment, Jackson; 10-nm gold-conjugated goat anti-mouse abs, Amersham.

1.2. Cell culture and transfection

The cells used were 293T (from human embryonic kidney) and SKNBE (from human bone marrow neuroblastoma). The cells were grown in DMEM medium supplemented with 10% foetal bovine serum, glutamine, penicillin/streptomycin and Na-pyruvate at 37 °C in 5% CO_2. SKNBE cells were transfected with Lipofectamine Plus (GIBCO) and 293T cells with 165 μM PEI

Table 1

Primers	Sequence
5′ *Bam*H1 cstb terminal primer	TATGGATCCATGATGTGTGGCGCGC
3′ *Eco*RI cstb terminal primer	CCGGAATTCTCAGAAGTAGGTTAGCTC
5′ cstbQ71P	GGGTGTTTCCACCCCTCCCTC
3′ cstbQ71P	GAGGGAGGGGTGGAAACACCC
3′ *Eco*RI cstb Δ68	ATAGAATTCTCACAAGTGCACACATTTTTC
3′ *Eco*RI cstb ΔTC	TAGGAATTCTCATGAGGGAGGTTCAAACA
3′ *Eco*RI cstb Δ64	TCAAGAATTCTCATTTTTCTTCGCCGACATCAAC
5′ *Bam*H1 cstb ΔE1	TATGGATCCTAGTGAAGTCTCAACTTGAAG
5′ cstb V59Q	CCAACTTCTTCATCAAGGTTGATCAGGGCGAAGAAAAATGTGTGC
3′ cstb V59Q	GCACACATTTTTCTTCGCCCTGATCAACCTTGATGAAGAAGTTGGG
3′ *Eco*RI cstb T87K	CCGGAATTCTCAGAAGTAGGTTAGCTCATCGTGCTTTTCTTTGTCCTTCTGGTAAGAGG
5′ *Bam*H1 cstb C3S	CTATGGATCCATGATGTCTGGCGCGCC
5′ cstb C64S	CGGCGAAGAAAAATCTGTGCACTTGAGGGTGTTTGAACCCC
3′ cstb C64S	GGGGTTCAAACACCCTCAAGTGCACAGATTTTTCTTCGCCG
5′ cstbV48D	CCTTCAGGAGACAGGTAGACGCCGGCACCAACTTCTTCATCAAGG
3′ cstbV48D	CCTTGATGAAGAAGTTCCTGCCGGCGTCTACCTGTCTCCTGAAGG
5′ cstbV48A	CCTTCAGGAGACAGGTAGCGGCCGGCACCAACTTCTTC
3′ cstbV48A	GAAGAAGTTGGTGCCGGCCGCTACCTGTCTCCTGAAGG
5′ cstbG50A	GGAGACAGGTAGTGGCCGCCACCAACTTCTTCATCAAGG
3′ cstbG50A	CCTTGATGAAGAAGTTGGTGGCGGCCACTACCTGTCTCC
5′ *Bam*H1 cstb G4R *Bss*HII [a]	GATCCATGATGTGTCG
3′ *Bam*H1 cstb G4R *Bss*HII[a]	CGCGCGACACATCATG
5′ cstbVG48/50A	GGAGACAGGTAGCGGCCGCCACCAACTTCTTCATCAAGG
3′ cstbVG48/50A	CCTTGATGAAGAAGTTGGTGGCGGCCGCTACCTGTCTCC
5′ *Xho*I cstb terminal primer [b]	TATCTCGAGGAATGATGTGTGGCGCGC
5′ *Xho*I cstb G4R[b]	TATCTCGAGGAATGATGTGTCGCGCGCCATCCG
5′ *Xho*I cstbC3S[b]	TATCTCGAGGAATGATGTCTGGCGCGCC
5′ *Nco*1-HA-polylinker [c]	CATGGCCTACCCCTACGACGTGCCCGACTACGCCTCCCTCGGATCCGGTACCCGGGCTCGAGCC
3′ *Nco*1-HA-polylinker[c]	GATCGGCTCGAGCCCGGGTACCGGATCCGAGGGAGGCGTAGTCGGGCACGTCGTAGGGGTAGGC
3′ *Xho*I cstb terminal primer	CGATTCTCGAGTCAGAAGTAGGTTAGCTCATCG

[a] The two complementary sequences were annealed and inserted directly into the *Bam*HI–*Bss*HII sites of the pRK7-HA-cstb vector.
[b] Primers for pEGFP-C1.
[c] The two complementary sequences were annealed and inserted directly into the *Nco*I–*Bam*HI sites of the pET16b vector (Novagen).

using 5 μg/ml plasmid (Sigma). Cells were grown for 16 h before harvesting. Rat cstb cDNA was used in all transfection experiments.

1.3. Cell lysis

Cells were harvested and washed in PBS. Lysis was (1) under non-denaturing conditions, in PBS containing 20% glycerol, 0.4 mM EDTA, 1 mM DTT, 0.5% NP40, antiprotease and anti-phosphatase cocktail (Sigma) (buffer 1); (2) under denaturing conditions, in PBS containing 1% SDS (buffer 2). The protein extracts were boiled 10 min and diluted in PBS containing antiprotease and anti-phosphatase cocktail (Sigma), to a final concentration of 0.1% SDS. The samples were sonicated and centrifuged 30 min at 13,000 rpm, 4 °C. The supernatants were stored at −80 °C. Protein concentration was determined using the Bio-Rad Protein Assay.

1.4. Immunoprecipitation experiments

Immunoprecipitation was carried out as previously described [10].

1.5. Redox experiments

The protein extracts were from cells lysed in buffer 1. pH curve: 60 μg protein extract was incubated 5 min on ice, in 100 mM Tris–HCl or 50 mM Na carbonate/bicarbonate buffers at the indicated pH. GSH curve: 60 μg protein extract was incubated 10 min at RT, in 100 mM Tris–HCl pH 7.5 with GSH at the indicated concentrations. H_2O_2 curve: 60 μg protein extract was incubated 20 min at RT, in H_2O_2 at the indicated concentrations. The reaction was stopped by addition of loading buffer (12 mM Tris–HCl pH 6.8, 5% glycerol, 1% SDS and 0.02% bromophenol blue) with or without 50 mM β-METOH, as indicated.

1.6. SDS-free size exclusion chromatography

Approximately 400 μg protein extract from 293T cells lysed in buffer 1 was loaded on Tricorn Superdex®75 PC 3.2/30 (Amersham) equilibrated with 50 mM Tris–HCl pH 7.5 and run at a flow rate of 0.1 ml/min. 50 μl Fractions were collected.

1.7. Protein identification by mass spectrometry

30 mg 293T protein extract was immunoprecipitated. The immunoprecipitate (ip) was loaded on gel without eluting from the gel beads. The bands were excised from the gel, reduced, alkylated using iodoacetamide, and digested with trypsin. The resulting fragments were extracted and analyzed by LC/MS on a Q-Tof Premier instrument (Waters, Corporation, Milford, MA, USA) coupled with a Waters 1065 HPLC apparatus (Waters Corporation). Peptides separation was carried out on a Proteus C18 (100×1 mm) column (Phenomenex, Foster City, CA, USA) using a linear gradient from 5% to 60% of 1% formic acid, 0.05% trifluoroacetic acid in CH_3CN over 50 min (flow rate 50 μl/min). Mass spectra were acquired over a *m/z* range from 400 to 2000. The resulting fragments were extracted, purified using C18 ZipTip (Millipore) and measured by MALDI-TOF mass spectrometry on a Biflex instrument (Bruker, Bremen).

1.8. Site-directed mutagenesis

WT and mutant CSTB sequences were inserted in the pRK7 vector containing one copy of the hemagglutinin tag sequence (pRK7-HA) upstream from the *Bam*HI site. The recombinants were inserted between the *Bam*HI and *Eco*RI sites. Mutagenesis was carried out by PCR amplification using the primers indicated in Table 1. wt and mutant sequences were inserted between the *Xho*I and *Eco*RI sites of the pEGFP-C1 vector (BD Biosciences Clontech). The pET16b-HA vector was generated from the pET16b vector (Novagen) by insertion of the hemagglutinin sequence upstream the insertion site.

1.9. Bacterial protein extracts

Escherichia coli BL21 (DE3) cells were transformed by electroporation and induced for 3 h with 0.5 mM IPTG (Sigma) before harvesting and lysing in buffer 1.

1.10. Preabsorption experiments

Anti-CSTB abs (at a final concentration of 24 μg/ml) or anti-HA(F-7) abs (at a final concentration of 0.28 μg/ml) were mixed with the protein extract from BL21 cells (with or without CSTB) at the final concentration of 9.5 mg/ml. Following a 1-h incubation at RT the protein extracts were centrifuged 10 min at 13,000 rpm. The supernatants were collected and analyzed by Western blot. The immunostaining was with anti-CSTB or -HA abs.

Immunofluorescence analysis, confocal microscopy, co-localization analysis and transmission electron microscopy were carried out as previously described [11,29].

2. Results

2.1. Cellular CSTB has a polymeric structure

The structural organization of endogenous (human) and transfected (rat) CSTB in the 293T cell line is analyzed in Fig. 1. The expected molecular weight (MW) for CSTB is approximately 12 kDa. In the absence of DTT, a complex pattern of

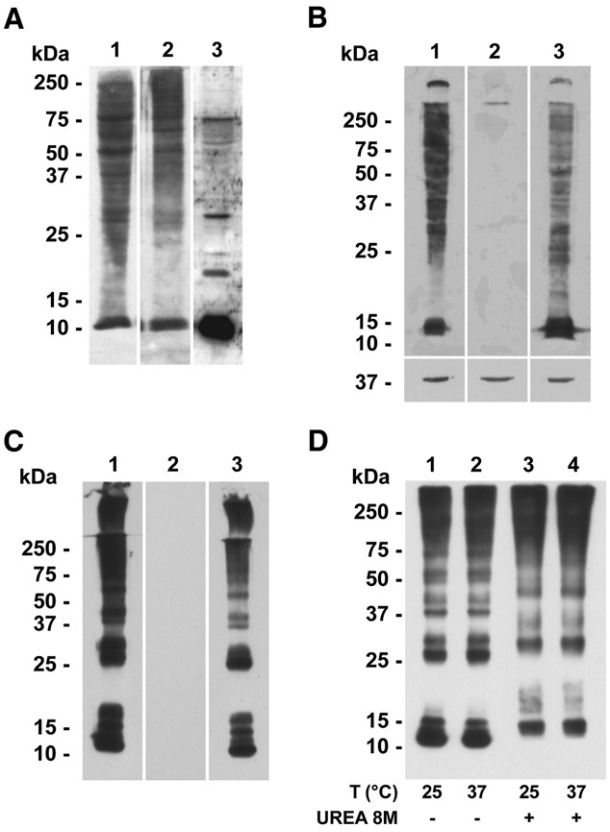

Fig. 1. Structural organization of cellular CSTB. Western blot analysis: (A) protein extract from 293T cells lysed without (buffer 1, lanes 1 and 3) and with (buffer 2, lane 2) 1% SDS and run in absence (lanes 1 and 2) and presence (lane 3) of 50 mM DTT. Staining with anti-CSTB abs. (B) Protein extract from cells lysed in buffer 1. Staining with anti-CSTB abs: untreated (lane 1), preabsorbed with *E. coli* protein extract expressing human CSTB (lane 2) or *E. coli* protein extract (lane 3). Lower panel: staining with anti-GAPDH abs. (C) Protein extract from 293T cells, transfected with the pRK7-HA vector containing rat *cstb* cDNA, lysed in buffer 2. Staining with anti-HA(F-7) abs: untreated (lane 1), preabsorbed with *E. coli* protein extract expressing rat HA-CSTB (lane 2) or *E. coli* protein extract (lane 3). (D) The same protein extracts as in panel C incubated 1 h as indicated. No reducing agents added. Staining with anti-HA(F-7) abs.

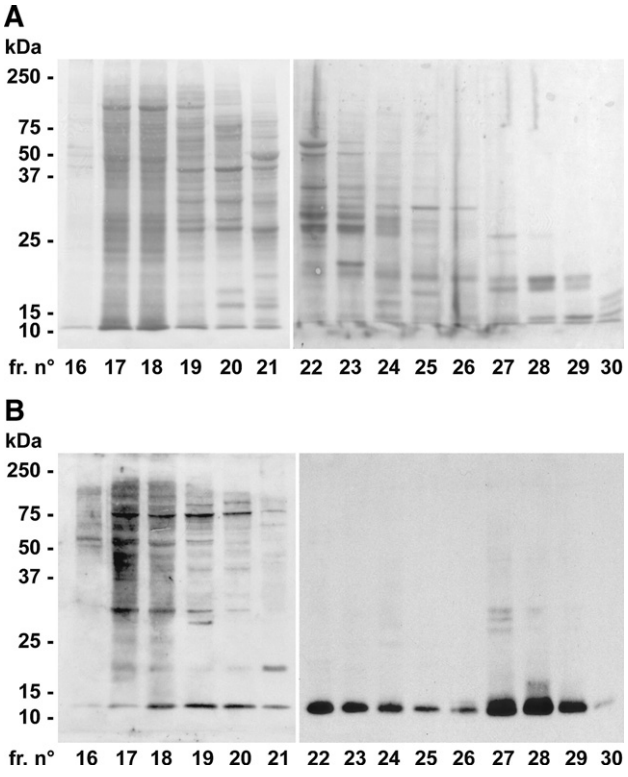

Fig. 2. SDS-free size exclusion chromatography of CSTB from a native protein extract of 293T cells analyzed on a Tricorn Superdex®75 column: fractions from the column loaded on SDS Laemmli gel without reducing agents and analyzed by Western blot. Fraction 17 contains the excluded peak of the column and from 19 onward the separation starts. (A) The size distribution of the proteins stained with Poinceau red shows the expected separation of the molecular weights in fractions 19–30. (B) Western blot stained with anti-CSTB abs.

bands ranging between 10 and 250 kDa is present in both lysates, with a similar distribution and intensity. The reducing condition increases the intensity of the 12-kDa band although some of the polymers are still detectable. To make sure that the high molecular weight components were real and not due to antibody background, we have checked the antibody specificity by preabsorption experiments. B shows that preabsorption of the anti-CSTB abs with human CSTB, synthesised in *E. coli*, cancels the endogenous signal. The same is true in C, where the 293T cells were transfected with rat HA-CSTB and preabsorption was carried out with rat HA-CSTB synthesised in *E. coli*. These results confirm the presence, *in vivo*, of a polymeric structure resistant to SDS denaturation (lane 2A) and sensitive to DTT treatment (lane3A) which may represent either co- or homopolymers of CSTB. The same polymeric pattern was obtained analyzing rat PC12 and B104 cells, human SKNBE and HeLa cells and, interestingly, *E. coli* transformed with a CSTB expressing construct (not shown). It should be noticed that *E. coli* does not express cystatin-like proteins and represents a background free system. Treatment with 8 M urea before SDS-PAGE does not denature CSTB polymers (panel D), although a few bands, in the intermediate molecular weight range, are no longer detectable. We conclude that the polymeric structure of CSTB is resistant to denaturation in 1% SDS and 8 M urea, and partially resistant to reducing agents. For simplicity, we will call "CSTB polymers" all CSTB high molecular weight species resistant to denaturation.

The native size of the high molecular mass CSTB components was examined submitting the protein extract from 293T cells to size fractionation (Fig. 2). The Western blot analysis of the fractions stained with anti-CSTB abs shows that low MW components, mainly monomers, are in fractions 21–30 (panel B). Fractions 27–30 correspond to the approximate MW of the CSTB monomer, dimer and trimer, suggesting that a small amount of CSTB is not bound to other proteins. Monomeric CSTB in fractions 21–26 is probably released from its interaction with cellular proteins upon SDS boiling and SDS-PAGE. In fact, native CSTB interacts with a number of proteins that increase its size on fractionation [10]. Polymeric CSTB is detectable in fractions 17–20, corresponding to the excluded peak of the column. The presence of the entire band ladder in the excluded region suggests that also the polymers interact with

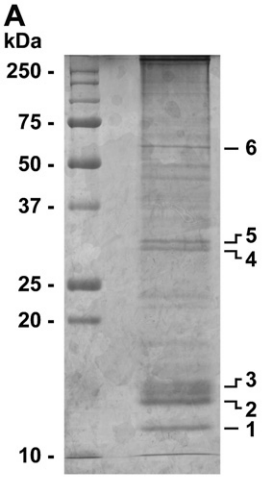

B

BAND 1			BAND 2			BAND 3		
MM (Exp)	PEPTIDE	MM (Th)	MM (Exp)	PEPTIDE	MM (Th)	MM (Exp)	PEPTIDE	MM (Th)
732,4	25-30 H	732,4	733,0	39-44 R	732,8	733,0	39-44 R	732,8
636,5	35-39 H	636,4	655,0	49-53 R	654,8	655,0	49-53 R	654,8
550,5	40-44 H	550,3	592,9	54-58 R	592,7	592,9	54-58 R	592,7
1325,9	45-56 H	1325,7	1223,6	60-70 R	1223,4	1223,6	60-70 R	1223,4
1421,9	57-68 H	1421,7	775,0	71-77 R	774,8	775,0	71-77 R	774,8
2457,6	69-89 H	2457,3	683,9	78-82 R	683,8	683,9	78-82 R	683,8
923,5	92-98 H	923,4	2444,1	83-101R	2443,7	924,3	106-112 R	924,0
			924,3	106-112 R	924,0			

BAND 4			BAND 5			BAND6		
MM (Exp)	PEPTIDE	MM (Th)	MM (Exp)	PEPTIDE	MM (Th)	MM (Exp)	PEPTIDE	MM (Th)
733,0	39-44 R	732,8	733,0	39-44 R	732,8	733,0	39-44 R	732,8
655,0	49-53 R	654,8	655,0	49-53 R	654,8	655,0	49-53 R	654,8
1223,6	60-70 R	1223,4	1223,6	60-70 R	1223,4	1223,6	60-70 R	1223,4
775,0	71-77 R	774,8	775,0	71-77 R	774,8	683,9	78-82 R	683,8
683,9	78-82 R	683,8	683,9	78-82 R	683,8	924,3	106-112 R	924,0
924,3	106-112 R	924,0	732,4	25-30 H	732,4	732,4	25-30 H	732,4
732,4	25-30 H	732,4	1325,9	45-56 H	1325,7	1421,9	57-68 H	1421,7
1325,9	45-56 H	1325,7	1421,9	57-68 H	1421,7	2457,6	69-89 H	2457,3
1421,9	57-68 H	1421,7	2457,6	69-89 H	2457,3			
2457,6	69-89 H	2457,3						

Fig. 3. Mass spectrometry analysis of the CSTB polymers. (A) Ip with anti-HA(F-7) abs from the same protein extract as in Fig. 1C. No reducing agents added to the sample. Gel stained with colloidal brilliant blue G (Sigma). Numbers on the right indicate the analyzed bands. (B) Mass spectrometry analysis. The position of each peptide within the CSTB sequence is shown. H refers to human and R to rat CSTB.

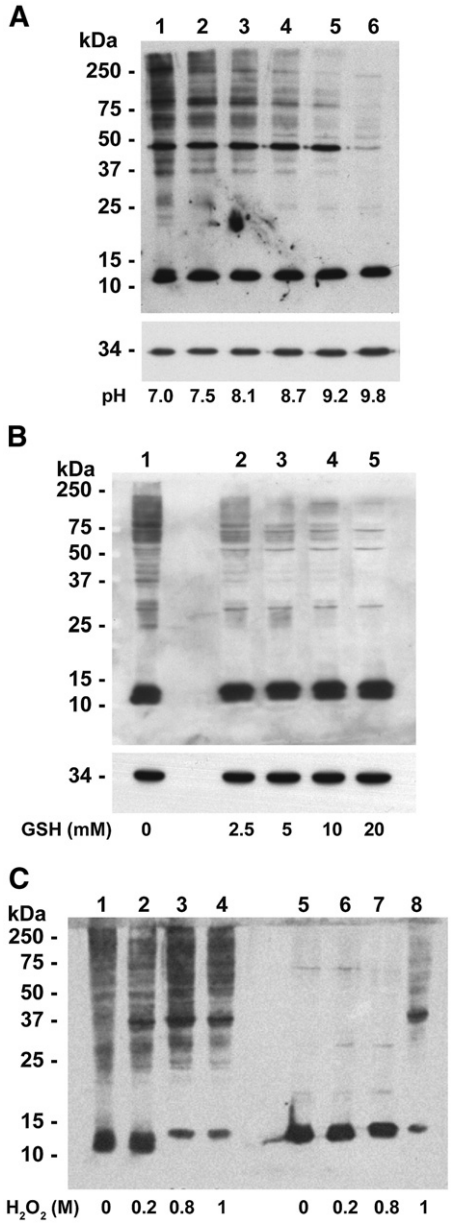

Fig. 4. Effect of pH, reducing and oxydising agents on CSTB polymers from 293T cells lysed in buffer 1. Staining with anti-CSTB abs. Lower panels in A and B: staining with anti-GAPDH abs. 60 μg protein extract were loaded on each lane. (A) pH curve as indicated. No reducing agents added to the samples. (B) Samples treated with increasing concentrations of GSH as indicated. No reducing agents added to the samples. (C) Samples treated with increasing concentrations of H_2O_2 as indicated. Lanes 1–4: minus reducing agents, lanes 5–8: plus reducing agents.

other proteins. We conclude that: (1) polymeric CSTB is present in the cells and is eluted in the excluded volume of the column; (2) protein interactions occur mainly with polymeric CSTB. The clear separation between low and high molecular mass components, present in different fractions of the column, shows that polymerization of CSTB is not an artefact due to SDS or self-assembly.

To distinguish between homo- and heteropolymers, the SDS denatured immunoprecipitated CSTB was analyzed by *in gel* digestion and mass spectrometry. The SDS-PAGE is shown in Fig. 3. The bands indicated in A were analyzed and the experimental results were compared to the theoretical molecular mass values (panel B). Bands 1, 2, 3 migrate at the position of endogenous and transfected monomers. Bands 4 and 5 migrate as homo- and hetero-trimers and band 6 as a pentamer. Protein modifications are not detectable although monomer, dimer and trimer migrate in multiple bands within the range of approximately 2 kDa. We envisage two possible reasons for this: (1) the N-terminal region of the protein (fragments 1–24) was not identified by mass spectrometric analysis, therefore the presence of modifications within the first 24 aa cannot be excluded. (2) The structure of the protein is unstable and shows conformational changes [19,30,31]. The identity between the experimental and theoretical molecular mass values confirms that the bands contain CSTB only, and that their position in the denaturing gel is not due to the interaction with other proteins. As we have transfected human 293T cells with rat CSTB and the rat and human sequences are different, we can distinguish the endogenous human from the transfected rat molecules (panel B and Fig. 6A). Both species are in polymeric and monomeric form and this can be explained by the interaction between endogenous and transfected CSTB that can be partially denaturated by boiling. We conclude that SDS-resistant CSTB polymers are not due to covalent interaction with proteins different from itself and that CSTB forms homopolymeric structures.

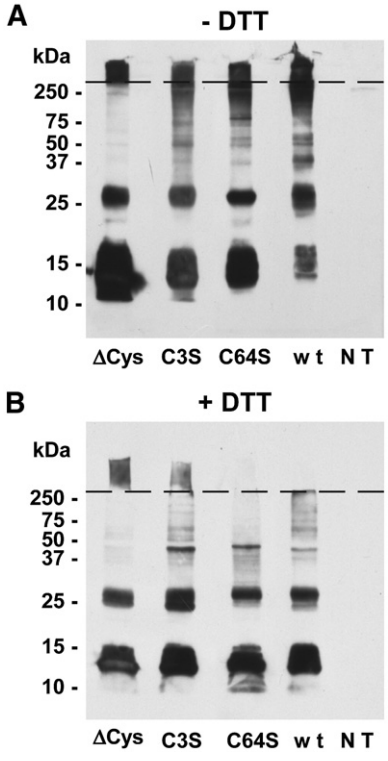

Fig. 5. Transfection of CSTB mutants in 293T cells lysed in buffer 2. Ip with anti-HA(F-7) abs of protein extracts from 293T cells transfected with wt and mutant constructs indicated under the lanes. NT refers to non-transfected cells. SDS polyacrylamide gels run minus (A) and plus (B) 200 mM DTT. Staining with anti-HA(Y11) abs. The dotted line indicates the position of the stacking region of the gel.

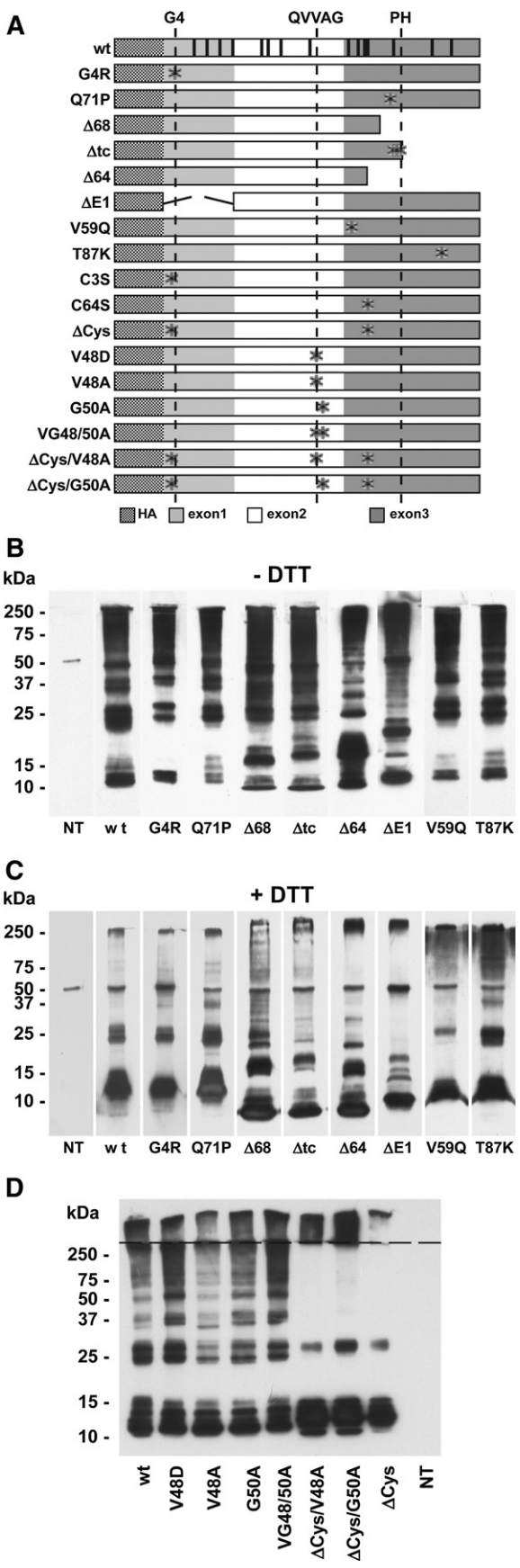

Fig. 4 analyzes the properties of polymers in relation to a treatment with reducing/oxydising agents. The effect of increasing pH on the polymeric structure is shown in panel A where polymers are barely detectable at pH 9.8. Glutathione at a concentration 2.5–20 mM decreases but does not eliminate the high MW CSTB bands (panel B). The effect of these treatments suggests that CSTB polymers are somewhat resistant to denaturation and that a combination of reducing and denaturing conditions are necessary to depolymerize the protein. Panel C shows the effect of H_2O_2 addition to a protein extract from 293T cells. As the concentration of H_2O_2 increases, we observe first an increase of the dimer band, followed by the trimer that becomes the dominant species at 1 M H_2O_2. This result suggests that, under oxydising conditions, the trimeric structure of CSTB is very stable. Under reducing conditions monomers are released from the high MW components up to a concentration of 0.8 M H_2O_2. The sample treated with 1.0 M H_2O_2 shows considerable resistance to denaturation of the trimer and of higher MW components suggesting the existence of irreversible hyperoxydated species, carrying sulphonylated, carbonylated or nitrated residues [32,33].

2.2. The cysteine-minus mutants of CSTB

The reactive thiol groups fulfil a sensory and regulatory role on proteins, in response to a defined redox environment. Most CSTB, including the human molecule, contain only one cysteine at position 3, while rodent CSTB has an additional cysteine at position 64 [4]. The phylogenetic conservation of Cys3 and the sensitivity of the high molecular weight species to the redox environment suggest that at least one cysteine is important. Thus, we have analyzed the structure of single and double cysteine substitution mutants of rat CSTB. The ips from protein extracts of cells transfected with these constructs are in Fig. 5, panels A and B. The banding pattern of the single substitution mutants is similar to that of the wt protein suggesting that the two cysteines present in the rat molecule are interchangeable. In

Fig. 6. Transfection of CSTB mutants in 293T cells lysed in buffer 2. (A) Structure of wt and mutant rat CSTB constructs. The vertical lines in the wt scheme indicate the position of amino acids which differ between rat and man. The asterisks indicate the position of the amino acid substitutions in the mutants. The dotted lines indicate the position of the phylogenetically conserved motives shown above. The mutants were constructed using the cystatin sequence alignments published by Rawlings and Barrett [4]. The natural mutants were G4R, Q71P, Δ68 and Δtc. Additional truncation mutants were Δ64 (stop codon at position 64) and ΔE1 (deletion of exon 1 encoding aa 1–22). Staniforth et al. [20] have shown that the chicken cystatin mutant I66Q forms dimers while the I102K generates monomers only. The I66Q is the chicken equivalent of human L68Q, from patients affected by the Icelandic type of amyloidosis [34]. Although CSTB and C belong to different families of cystatins, their phylogenetic conservation allows the construction of equivalent mutants for the two species. V59Q and T87K (panel A) are derived from I66Q and I102K mutants respectively. (B, C) Ip with anti-HA(F-7) abs of protein extracts from 293T cells transfected with wt and mutant constructs indicated under the lanes. NT refers to non-transfected cells. SDS polyacrylamide gels run minus (B) and plus (C) 200 mM DTT. Staining with anti-HA(Y11) abs. Panels B and C are a pool of different experiments, each one carried out with its own NT and wt controls. (D) Protein extracts from 293T cells transfected with single and multiple substitution mutants of loop I. No reducing agents added to the samples. Staining with anti-HA (F-7) abs. The dotted line indicates the position of the stacking region of the gel.

contrast, the ΔCys mutant shows mainly monomers and dimers in addition to high MW polymers stacked in the high portion of the gel. The oligomers in the middle MW range are barely detectable. The addition of 200 mM DTT (B) to C3S, C64S and wt CSTB decreases the amount of protein in the stacking gel and releases components migrating in the middle MW range. The ΔCys mutant does not respond to DTT addition. We can conclude that cysteines are not necessary to form dimers, and that neither the phylogenetically conserved Cys 3 nor Cys 64 is necessary to the formation of high MW species. However, reactive thiol groups seem to be important to stabilize the intermediate MW species which are clearly visible and stable when at least one cysteine is present in the sequence. CSTA and chicken cystatin dimers generated *in vitro* by 3D domain swapping have been described by Staniforth et al. [20] as the initial step to the formation of amyloid fibers. Since CSTA belongs to the same family as CSTB, the dimer that we observe *in vivo* may have a similar origin, implicating hydrophobic interactions.

2.3. Structural organization of CSTB natural EPM1 mutants

We have analyzed the structural organization of a number of CSTB mutants including those isolated from EPM1 patients (Fig. 6). *In vivo* all CSTB mutants generate high MW structures (panel B). Differences in the banding patterns are mainly due to the different MW of the constructs. In agreement with the experiments shown in Fig. 5, the addition of 200 mM DTT is not sufficient to depolymerize CSTB completely (panel C). Both carboxyl- and amino-terminus deletion mutants seem to polymerize very efficiently. Accordingly, fast fibrillation of the N-terminal fragment in comparison to the wild type was observed by Rabzelj et al. [35]. In contrast to the results obtained by Staniforth et al. [20], the V59Q and T87K substitutions generate high MW components, suggesting a difference between the two polymerization processes. We conclude that none of the mutations analyzed interferes with the process of polymerization of CSTB *in vivo*.

According to Staniforth et al. [20], aa substitutions in the QVVAG loop of cystatins do not allow polymerization of the molecule. We have generated single and double substitution mutants of this region to see whether *in vivo* polymerization requires the integrity of loop I. The mutant V48D corresponds to the chicken mutant V55D of Staniforth et al. [20]. We have also mutated amino acids at the most highly conserved sites of the QVVAG loop: V48A, G50A and VG48/50A. The substitutions at aa positions 48 and 50 were also inserted in the cysteine-minus constructs (ΔCys/V48A and ΔCys/G50A). The distribution of the CSTB bands in all mutants is similar to that of the wt protein with the exception of the cysteine-minus constructs that show monomers, dimers and bands larger than 250 kDa as dominant species, while the intermediate forms are barely detectable (panel D).

We conclude that aa substitutions in loop I do not alter the polymerizing capacity of CSTB *in vivo*. These results, in contrast with those obtained by Staniforth et al. [20] *in vitro*, may be due to the presence, *in vivo*, of chaperon or other proteins involved in the polymerization process [36].

2.4. Expression of CSTB and its mutants in SKNBE cells

Since 293T cells tend to form foci during growth and are detached from the plate surface by the fixation procedure, we have chosen SKNBE neuroblastoma cells for microscopic analysis. The phenotype induced by expression of rat CSTB and its mutants in SKNBE cells was analyzed by immunofluorescence confocal

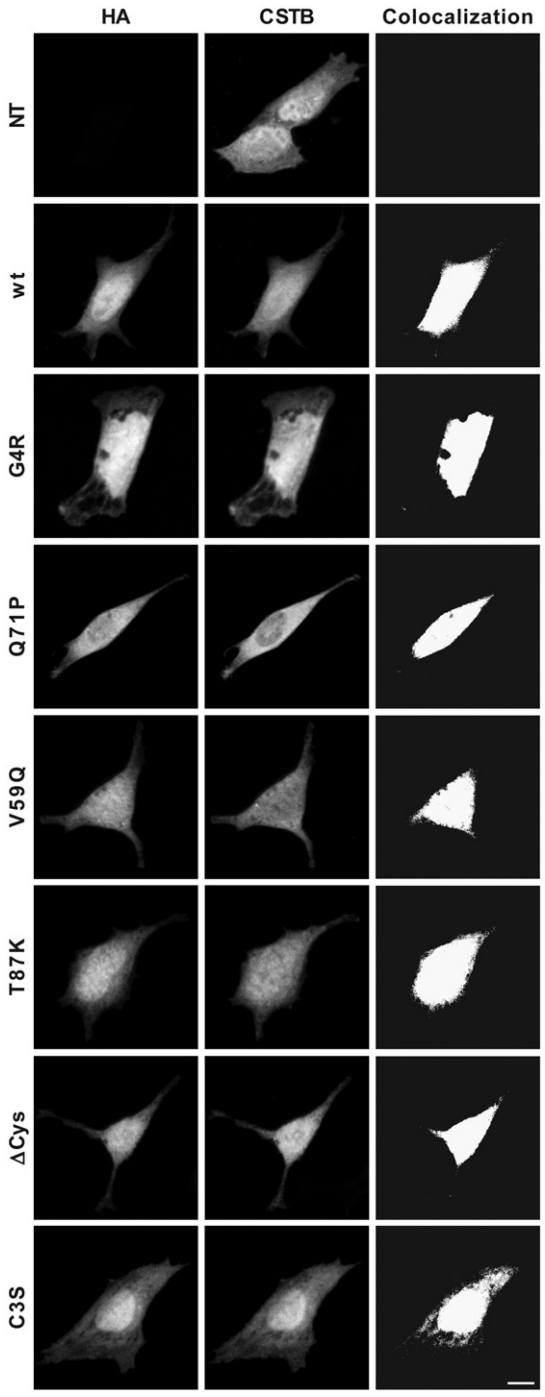

Fig. 7. Expression of CSTB. 24-h transfection of SKNBE cells with wt and mutant CSTB constructs: Confocal microscopy analysis of SKNBE cells transfected with wt and mutant CSTB as indicated: point mutations and cysteine substitution mutants are stained with anti-CSTB and anti-HA abs. Colocalization is shown. Scale bar: 5 μm.

microscopy (Fig. 7). The distribution of the wt protein is similar in transfected and non-transfected SKNBE cells. The localization of the protein is mainly nuclear although it is detectable also in the cytoplasm [28,37]. Following 24-h transfection, the localization of the substitution mutants is similar to that of wt rat CSTB. In contrast, the carboxy- and amino-terminus deletion mutants show a different distribution: the staining with anti-HA abs is barely detectable in the nuclear compartment and is strong in the cytoplasm (Fig. 8). Furthermore, the signal is concentrated in randomly distributed aggregates of variable size and number, similar to the cytoplasmic inclusion bodies described by Rajan et al. [49]. In some cases the aggregates are numerous and small (Δ68), in other cases we see large aggregates which may result from the confluence of small ones (Δ64 and ΔE1). In agreement with the nuclear presence of the endogenous protein, the same cells are stained by the anti-CSTB abs both in the nucleus and in the cytoplasm, and aggregated forms are also detected.

The EM analysis of cells transfected 24 h with rat wt CSTB and two deletion mutants is shown in Fig. 9. In agreement with our previous data [37], wt CSTB does not coincide with defined cellular structures. The gold particles show a regular distribution in the nucleus and in the cytoplasm, outside of the known cellular organelles. The pattern generated by the Δ68 and Δtc mutants is different from that of wt CSTB. The protein appears highly concentrated in some regions of the cytoplasm. The alignment of granules that we have observed in numerous aggregate containing cells is interesting [38]. The other deletion mutants analyzed showed a similar cellular distribution of CSTB (not shown).

We have carried out a time course of transfection up to 7 days in order to study the rate of aggregate formation throughout this period (Fig. 10). The ΔCys mutant, that seemed to modify the polymerization pattern of CSTB, and two natural EPM1 mutants were chosen for this experiment. The proportion of transfected cells is relatively constant up to 7 days when, in most samples, a decrease, possibly due to death, is detectable. The green fluorescent protein (EGFP) alone does not produce aggregates up to 7 days after transfection (panel A). The wt CSTB fusion construct starts generating aggregates 48 h after transfection and the number of positive cells increases gradually for 7 days, when approximately 40% of the transfected cells contain CSTB inclusions (panel B). The G4R mutant shows a steeply growing curve where, from days 5 to 7, 70–90% of the transfected cells contain aggregates (panel C). Twenty-four hours after transfection, the Δ68 fusion generates aggregates already in 20% of the cells (panel D). At day 5 almost 100% of the cells contain aggregates. The ΔCys fusion does not produce detectable aggregates until day 7, when approximately 30% of the transfected cells are affected (panel E). This result is interesting as we have seen that ΔCys is the only mutant altering the polymerization pattern of CSTB (Fig. 5). The delayed appearance of aggregates could be due to the presence of endogenous

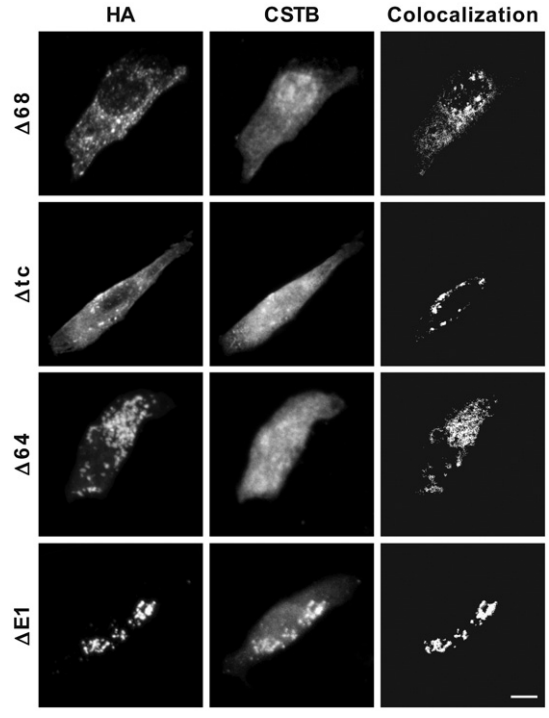

Fig. 8. Expression of CSTB. 24-h Transfection of SKNBE cells with deletion mutants of CSTB as indicated. Confocal microscopy analysis as in Fig. 7.

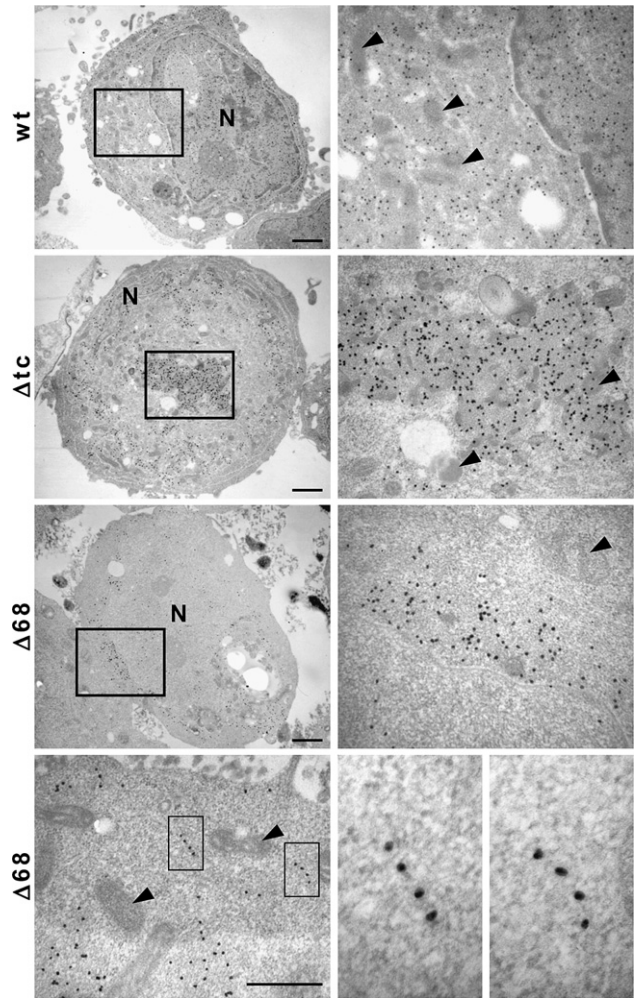

Fig. 9. EM analysis of SKNBE cells transfected with wild-type and two CSTB natural mutants as indicated. N: nucleus; arrows: mitochondria; rectangles: regions shown on the right in 5× magnification; scale bar: 1 μm.

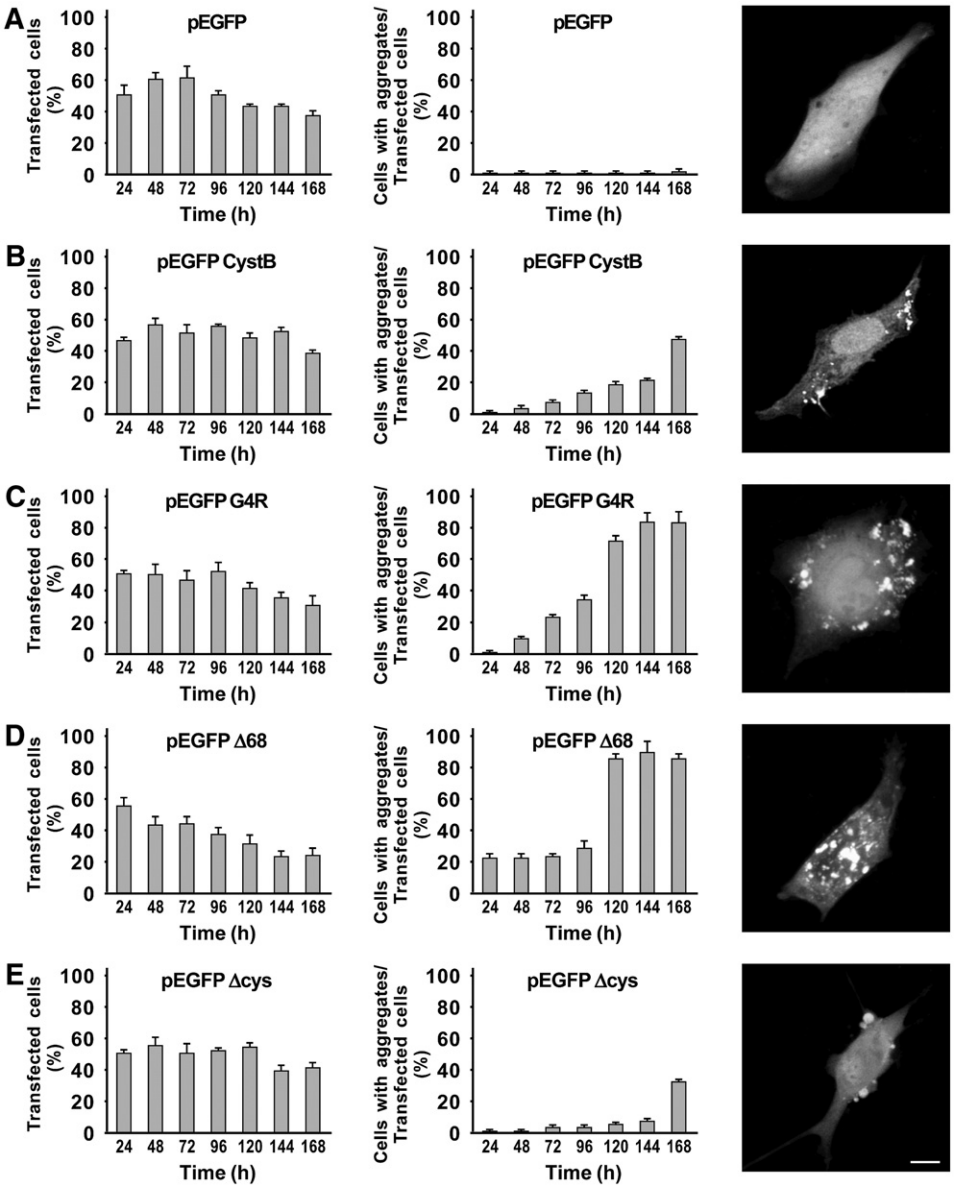

Fig. 10. Time course of transfection of SKNBE cells with pEGFP fusion constructs of wt and mutant CSTB. The percentage of cells containing CSTB aggregates is calculated as the ratio between aggregate containing and transfected cells and shown on the left. The statistical significance of the differences between the experimental points was evaluated by Student's *t*-test. Fluorescent aggregates generated by the CSTB fusion proteins are shown on the right of the histograms. The transfected constructs are indicated over each histogram. scale bar: 5 μm.

wild-type CSTB that, within a week, may trigger their formation. In fact, human CSTB contains the cysteine that may be important in aggregate formation.

3. Discussion

CSTB belongs to a highly conserved family of antiproteases, some of which have been associated with amyloidosis. So far, CSTB has been described as a protein monomeric *in vivo* and prone to amyloid fiber formation *in vitro* [17]. Manning and Colòn [39] have described a number of proteins characterized by high kinetic stability and resistance to SDS denaturation with a structure containing disulfide bonds, oligomeric interfaces and bound metals. These features are present in CSTB polymers that bind copper as well ([40], R. Di Giaimo, E. Cipollini, M. Melli unpublished observation). The exceptional resistance of CSTB polymers to SDS and 8M urea and the response to modifications of the redox conditions [32] are similar to those shown by oligomers from amyloid plaques of Alzheimer's disease patients [41].

The SDS-free size fractionation column of the native protein extract confirms the presence in the cell of polymers containing CSTB. A protein that interacts with partners of different MW in a native extract does not reflect the size of the protein itself. In fact, the prevalence of monomers in the linear part of the column and of variable size polymers in the high MW fractions, is in agreement with the interaction of CSTB with different proteins. In addition, the Western blot analysis shows clearly the presence in the excluded peak of the column, of SDS resistant CSTB polymers separate from monomers and dimers and the

mass spectrometry analysis shows that they are homopolymers [42,43].

Several authors have suggested that oligomerization through 3D domain swapping may represent an important step on the *in vitro* generation of oligomers [44–47]. Staniforth et al. [20] and Kokalj et al. [9] have proposed a model of *in vitro* growth by dimeric addition for cystatin amyloid fibers. We find that CSTB polymers *in vivo* grow by monomer addition. We can conclude that the process of polymerization *in vivo* and *in vitro* is different. The presence, *in vivo*, of chaperon-like and/or redox response proteins may be important to this process [32,36].

A diagnostic marker of amyloid fibers is the birefringence on polarized light, following congo red staining [19]. CSTB aggregates, stained with congo red, do not show this effect in 24-h transfection, suggesting that they do not contain amyloid fibers (not shown). It is worth noting that many prion diseases lack cerebral plaques that stain with amyloid specific dyes [48]. Cytoplasmic inclusion bodies have been described by Rajan et al. [49]. These aggregates are called aggresomes when they localize near the microtubule organizing center, through a process mediated by a dynein/dynactin retrograde transport. Our results do not allow a distinction between the two types of protein inclusions as their cellular localization seems to be variable. However, both types of aggregates are described in neurodegenerative disorders such as Parkinson's, Alzheimer's, ALS and Pick's diseases [50].

A regulatory role of cysteine(s) on the stability of the intermediate MW components, together with the evidence on the toxicity of oligomers in neurodegeneration, correlates with the late appearance of aggregates in cells transfected with the cysteine-minus mutant (Fig. 10) [41,48,53,54]. Amyloid-like proteins in yeast are physiological [55,56] and Berson et al. [57] have shown that amyloid-like fibril formation is physiological in man as well. *E. coli* and *Salmonella* form amyloid-like extracellular fibrils orchestrated by two different operons [58]. In synthesis, we may say that fibril formation is an evolutionary conserved mechanism for creating biologically active quaternary structures [59]. We propose that polymeric CSTB can also be classified as a protein whose properties are beneficial to the cell but prone to toxic aggregate formation when overexpressed.

Finally, our results suggest that the neurodegeneration observed in EPM1 patients heterozygous for both promoter and point mutations is caused by the expression of the mutant protein which is stable and tends to generate aggregates. This is in agreement with a previous suggestion by Rabzelj et al. [35] and Ceru et al. [60]. On the other hand, previous work casts doubts on the absence of antiprotease activity as a cause of EPM1 [24,51]. As CSTB interacts with a number of cytoskeletal proteins, we have proposed a cytoskeletal function for it [10,11] which may be important in neuronal signal transmission [52].

Acknowledgments

We are very grateful to Dr. F. Sparla and Dr. P. Trost for helping with the column fractionation procedure and for the discussion of the results; to Dr. B. Howes and Dr. A. Algeri for reading the manuscript.

This work was supported by Telethon grant GGP030248, partly by a grant from the Italian Ministry of Technology and Scientific Research and by a grant from FIRB Neuroscienze RBNE01WY7P.

References

[1] A.J. Barret, H. Kirschke, Cystatin, the egg white inhibitor of cysteine proteinases, Methods Enzymol. 80 (1981) 771.
[2] M. Jarvinen, A. Rinne, Human spleen cysteine proteinase inhibitor. Purification, fractionation into isoelectric variants and some properties of the variants, Biochim. Biophys. Acta 708 (1982) 210.
[3] V. Turk, W. Bode, The cystatins: proteins inhibitors of cysteine proteinases, FEBS Lett. 285 (1991) 213.
[4] N.D. Rawlings, A.J. Barrett, Evolution of proteins of the cystatin superfamily, J. Mol. Evol. 30 (1990) 60–71.
[5] W.M. Brown, K.M. Dziegielewska, Friends and relations of the cystatin superfamily—new members and their evolution, Protein Sci. 6 (1997) 5–12.
[6] A.E. Lehesjoki, Molecular background of progressive myoclonus epilepsy, EMBO J. 22 (2003) 3473–3478.
[7] M. Stubbs, B. Laber, W. Bode, R. Huber, R. Jerala, B. Lenarcic, V. Turk, The refined 2.4A X-ray crystal structure of recombinant human stefin B in complex with the cysteine proteinase papain: a novel type of proteinase inhibitor interaction, EMBO J. 9 (1990) 1939–1947.
[8] R. Janowski, M. Kozak, E. Jankowska, Z. Grzonka, A. Grubb, M. Abrahamson, M. Jaskolski, Human cystatin C, an amyloidogenic protein, dimerizes through three-dimensional domain swapping, Nat. Struct. Biol. 8 (2001) 316–320.
[9] S. Jenko Kokalj, G. Guncar, I. Stern, G. Morgan, S. Rabzelj, M. Kenig, R.A. Staniforth, J.P. Waltho, E. Zerovnik, D. Turk, Essential role of proline isomerization in stefin B tetramer formation, J. Mol. Biol. 9 (2007) 1569–1579.
[10] R. Di Giaimo, M. Riccio, S. Santi, C. Galeotti, D.C. Ambrosetti, M. Melli, New insights into the molecular basis of progressive myoclonus epilepsy (EPM1): a multiprotein complex with cystatin B, Hum. Mol. Genet. 11 (2002) 2941–2950.
[11] M. Riccio, S. Santi, M. Dembic, R. Di Giaimo, E. Cipollini, E. Costantino-Ceccarini, D.C. Ambrosetti, N.M. Maraldi, M. Melli, Cell-specific expression of the epm1 (cystatin B) gene in developing rat cerebellum, Neurobiol. Dis. 20 (2005) 104–114.
[12] D. Keppler, Towards novel anti-cancer strategies based on cystatin functions, Cancer Lett. 235 (2006) 159–176.
[13] L.A. Bobek, M.J. Levine, Cystatins-inhibitors of cysteine proteinases, Crit. Rev. Oral Biol. Med. 3 (1987) 307–332.
[14] C. Lefebvre, C. Cocquerelle, F. Vandenbulcke, D. Hot, L. Huot, L. Lemoine, M. Salzet, Transcriptomic analysis in the leech *Theromyzon tessulatum*: involvement of cystatin B in innate immunity, Biochem. J. 380 (2004) 617–625.
[15] K. Ii, H. Ito, E. Kominami, A. Hirano, Abnormal distribution of cathepsin proteinases and endogenous inhibitors (cystatins) in the hippocampus of patients with Alzheimer's disease, parkinsonism–dementia complex on Guam, and senile dementia and in the aged, Virchows Arch., A Pathol. Anat. Histopathol. 423 (1993) 185–194.
[16] T. Suzuki, S. Hashimoto, N. Toyoda, S. Nagai, N. Yamazaki, H.Y. Dong, J. Sakai, T. Yamashita, T. Nukiwa, K. Matsushima, Comprehensive gene expression profile of LPS-stimulated human monocytes by SAGE, Blood 96 (2000) 2584–2591.
[17] E. Zerovnik, M. Pompe-Novak, M. Skarabot, M. Ravnikar, I. Musevic, V. Turk, Human stefin B readily forms amyloid fibrils *in vitro*, Biochim. Biophys. Acta 1594 (2002) 1–5.
[18] S. Jenko, M. Skarabot, M. Kenig, G. Guncar, I. Musevic, D. Turk, E. Zerovnik, Different propensity to form amyloid fibrils by two homologous proteins—human stefins A and B: searching for an explanation, Proteins 55 (2004) 417–425.
[19] M.R. Nilsson, Techniques to study amyloid fibril formation *in vitro*, Methods 34 (2004) 151–160.

[20] R.A. Staniforth, S. Giannini, L.D. Higgins, M.J. Conroy, A.M. Hounslow, R. Jerala, C.J. Craven, J.P. Waltho, Three-dimensional domain swapping in the folded and molten-globule states of cystatins, an amyloid-forming structural superfamily, EMBO J. 20 (2001) 4774–4781.
[21] A. Sanders, C. Jeremy Craven, L.D. Higgins, S. Giannini, M.J. Conroy, A.M. Hounslow, J.P. Waltho, R.A. Staniforth, Cystatin forms a tetramer through structural rearrangement of domain-swapped dimers prior to amyloidogenesis, J. Mol. Biol. 336 (2004) 165–178.
[22] P. Genton, Unverricht–Lundborg disease (PME1), Rev. Neurol. (Paris) 162 (2006) 819–826.
[23] R. Eldridge, M. Iivanainen, R. Stern, T. Koerber, B.J. Wilderý`, 'Baltic' myoclonus epilepsy: hereditary disorder of childhood made worse by phenytoin, Lancet 8 (1983) 838–842.
[24] S.F. Berkovic, A. Mazarib, S. Walid, M.Y. Neufeld, J. Manelis, Y. Nevo, A.D. Korczyn, J. Yin, L. Xiong, M. Pandolfo, J.C. Mulley, R.H. Wallace, A new clinical and molecular form of Unverricht–Lundborg disease localized by homozygosity mapping, Brain 128 (2005) 652–658.
[25] G. Coppola, C. Criscuolo, G. De Michele, S. Striano, F. Barbieri, P. Striano, A. Perretti, L. Santoro, V. Brescia Morra, F. Sacca, V. Scarano, A.P. D'A damo, S. Banfi, P. Gasparini, F.M. Santorelli, A.E. Lehesjoki, A. Filla, Autosomal recessive progressive myoclonus epilepsy with ataxia and mental retardation, J. Neurol. 252 (2005) 897–900.
[26] R. Lafreniere, D. Rochefort, N. Chrretien, J. Rommens, J. Cochius, R. Kalviainen, U. Nousiainen, G. Patry, K. Farrel, B. Soderfeldt, A. Federico, B. Hale, O. Cossio, T. Soresen, M. Pouliot, T. Kmiec, P. Uldal, J. Janszky, M. Pranzatelli, F. Andermann, E. Anderman, G. Rouleau, Unstable insertion in the 5' flanking region of the cystatin B gene is the most common mutation in progressive myoclonus epilepsy type 1, EPM1, Nat. Genet. 15 (1997) 298–302.
[27] K. Virtaneva, E. D'Amato, J. Miao, M. Koskiniemi, R. Norio, G. Avanzini, S. Franceschetti, R. Michelucci, C.A. Tassinari, S. Omer, L.A. Pennacchio, R.M. Myers, J.L. Dieguez-Lucena, R. Krahe, A. de la Chapelle, A.E. Lehesjoki, Unstable minisatellite expansion causing recessively inherited myoclonus epilepsy, EPM1, Nat. Genet. 15 (1997) 393–396.
[28] K. Alakurtti, E. Weber, R. Rinne, G. Theil, G.J. de Haan, D. Lindhout, P. Salmikangas, P. Saukko, U. Lahtinen, A.E. Lehesjoki, Loss of lysosomal association of cystatin B proteins representing progressive myoclonus epilepsy, EPM1, mutations, Eur. J. Hum. Genet. 13 (2005) 208–215.
[29] M. Riccio, M. Dembic, C. Cinti, S. Santi, Multifluorescence labeling and colocalization analysis, Methods Mol. Biol. 285 (2004) 171–177.
[30] E. Zerovnik, R. Jerala, L. Kroon-Zitko, R.H. Pain, V. Turk, Intermediates in denaturation of a small globular protein, recombinant human stefin B, J. Biol Chem. 267 (1992) 9041–9046.
[31] E. Zerovnik, R. Jerala, L. Kroon-Zitko, V. Turk, K. Lohner, Characterization of the equilibrium intermediates in acid denaturation of human stefin B, Eur. J. Biochem. 245 (1997) 364–372.
[32] S.O. Kim, K. Merchant, R. Nudelman, W.F. Beyer Jr., T. Keng, J. De Angelo, A. Hausladen, J.S. Stamler, OxyR: a molecular code for redox-related signaling, Cell 109 (2002) 383–396.
[33] P. Ghezzi, V. Bonetto, Redox proteomics: identification of oxidatively modified proteins, Proteomics 3 (2003) 1145–1153.
[34] E. Levy, M. Jaskolski, A. Grubb, The role of cystatin C in cerebral amyloid angiopathy and stroke: cell biology and animal models, Brain Pathol. 16 (2006) 60–70.
[35] S. Rabzelj, V. Turk, E. Zerovnik, *In vitro* study of stability and amyloid-fibril formation of two mutants of human stefin B (cystatin B) occurring in patients with EPM1, Protein Sci. 14 (2005) 2713–2722.
[36] P.J. Muchowski, J.L. Wacker, Modulation of neurodegeneration by molecular chaperones, Nat. Rev., Neurosci. 6 (2005) 11–22.
[37] R. Di Giaimo, S. Pianetti, P.P. Calmieri, M. Melli, S. Santi, Nuclear localization of cystatin B, the cathepsin inhibitor implicated in myoclonous epilepsy (EPM1), Exp. Cell Res. 262 (2001) 84–94.
[38] V.V. Speransky, K.L. Taylor, H.K. Edskes, R.B. Wickner, A.C. Steven, Prion filament networks in [URE3] cells of *Saccharomyces cerevisiae*, J. Cell Biol. 153 (2001) 1327–1336.
[39] M. Manning, W. Colòn, Structural basis of protein kinetic stability: resistance to sodium dodecyl sulfate suggests a central role for rigidity and a bias toward beta-sheet structure, Biochemistry 43 (2004) 11248–11254.
[40] E. Zerovnik, K. Skerget, M. Tusek-Znidaric, C. Loeschner, M.W. Brazier, D.R. Brown, High affinity copper binding by stefin B (cystatin B) and its role in the inhibition of amyloid fibrillation, FEBS J. 273 (2006) 4250–4263.
[41] D.M. Walsh, I. Klyubin, J.V. Fadeeva, W.K. Cullen, R. Anwyl, M.S. Wolfe, M.J. Rowan, D.J. Selkoe, Naturally secreted oligomers of amyloid beta protein potently inhibit hippocampal long-term potentiation *in vivo*, Nature 416 (2002) 535–539.
[42] D.M. Walsh, M. Townsend, M.B. Podlisn, G.M. Shanka, J.V. Fadeev, O.E. Agnaf, D.M. Hartley, D.J. Selkoe, Certain inhibitors of synthetic amyloid beta-peptide (Abeta) fibrillogenesis block oligomerization of natural Abeta and thereby rescue long-term potentiation, J. Neurosci. 25 (2005) 2455–2462.
[43] S. Lesne, M.T. Koh, L. Kotilinek, R. Kayed, C.G. Glabe, A. Yang, M. Gallagher, K.H. Ashe, A specific amyloid-beta protein assembly in the brain impairs memory, Nature 440 (2006) 352–357.
[44] K.J. Knaus, M. Morillas, W. Swietnicki, M. Malone, W.K. Surewicz, V.C. Yee, Crystal structure of the human prion protein reveals a mechanism for oligomerization, Nat. Struct. Biol. 8 (2001) 770–774.
[45] R. Janowski, M. Abrahamson, A. Grubb, M. Jaskolski, Domain swapping in N-truncated human cystatin C, J. Mol. Biol. 341 (2004) 151–160.
[46] M. Nilsson, X. Wang, S. Rodziewicz-Motowidlo, R. Janowski, V. Lindstrom, P. Onnerfjord, G. Westermark, Z. Grzonka, M. Jaskolski, A. Grubb, Prevention of domain swapping inhibits dimerization and amyloid fibril formation of cystatin C: use of engineered disulfide bridges, antibodies, and carboxymethylpapain to stabilize the monomeric form of cystatin C, J. Biol. Chem. 279 (2004) 24236–24245.
[47] M. Wahlbom, X. Wang, V. Lindström, E. Carlemalm, M. Jaskolski, Anders Grubb, Fibrillogenic oligomers of human cystatin c are formed by propagated domain swapping, J. Biol. Chem. 282 (25) (June 22 2007) 18318–18326.
[48] D.A. Harris, H.L. True, New insights into prion structure and toxicity, Neuron 50 (2006) 353–357.
[49] R.S. Rajan, M.E. Illing, N.F. Bence, R.R. Kopito, Specificity in intracellular protein aggregation and inclusion body formation, Proc. Natl. Acad. Sci. U. S. A. 98 (2001) 13060–13065.
[50] R.R. Kopito, Aggresomes, inclusion bodies and protein aggregation, Trends Cell Biol. 10 (2000) 524–530.
[51] M.K. Houseweart, L.A. Pennacchio, A. Vilaythong, C. Peters, J.L. Noebels, R.M. Myers, Cathepsin B but not cathepsins L or S contributes to the pathogenesis of Unverricht–Lundborg progressive myoclonus epilepsy (EPM1), J. Neurobiol. 56 (2003) 315–327.
[52] S. Franceschetti, G. Sancini, A. Buzzi, S. Zucchini, B. Paradiso, G. Magnaghi, C. Frassoni, M. Chikhladze, G. Avanzini, M. Simonato, A pathogenetic hypothesis of Unverricht–Lundborg disease onset and progression, Neurobiol. Dis. 25 (2006) 675–685.
[53] S.R. Collins, A. Douglass, R.D. Vale, J.S. Weissman, Mechanism of prion propagation: amyloid growth occurs by monomer addition, PLoS Biol. 2 (2004) 1582–1590.
[54] C.M. Dobson, Protein folding and misfolding, Nature 426 (2003) 884–890.
[55] S. Lindquist, Mad cows meet psichotic yeast: the expansion of the prion hypothesis, Cell 89 (1997) 495–498.
[56] M.F. Tuite, B.S. Cox, Propagation of yeast prions, Nat. Rev., Mol. Cell. Biol. 4 (2003) 878–890.
[57] J.F. Berson, A.C. Theos, D.C. Harper, D. Tenza, G. Raposo, M.S. Marks, Proprotein convertase cleavage liberates a fibrillogenic fragment of a resident glycoprotein to initiate melanosome biogenesis, J. Cell Biol. 161 (2003) 521–533.
[58] M.R. Chapman, L.S. Robinson, J.S. Pinkner, R. Roth, J. Heuser, M. Hammar, S. Normark, S.J. Hultgren, Role of *Escherichia coli* curli operons in directing amyloid fiber formation, Science 295 (2002) 851–855.
[59] J.W. Kelly, W.E. Balch, Amyloid as a natural product, J. Cell Biol. 12 (2003) 461–462.
[60] S. Ceru, S. Rabzelj, N. Kopitar-Jerala, V. Turk, E. Zerovnik, Protein aggregation as a possible cause for pathology in a subset of familial Unverricht–Lundborg disease, Med. Hypotheses 64 (2005) 955.